

DIFFUSION OF HYDROGEN ATOMS FROM Si_3N_4 DIELECTRIC SUBSTRATES INTO AMORPHOUS AND POLYCRYSTALLINE Si AND Ge FILMS

© 2024 L. V. Arapkina*, K. V. Chizh, D. B. Stavrovskii, V. P. Dubkov,
M. S. Storozhevykh, V. A. Yuryev

A. M. Prokhorov General Physics Institute of the Russian Academy of Sciences, 38 Vavilov Street, Moscow, 119991, Russia

Received July 28, 2023

Revised September 28, 2023

Accepted September 29, 2024

Abstract. The results of RHEED and FTIR investigation of polycrystalline and amorphous Si and Ge films deposited on dielectric $\text{Si}_3\text{N}_4/\text{SiO}_2/\text{Si}$ (001) substrates are presented. A decrease in the intensity of the IR absorption bands of N–H vibrations in the Si_3N_4 layers is observed, which is associated with the migration of H atoms from Si_3N_4 into the growing Si and Ge films. This transfer occurs at 30 °C and increases with increasing temperature (30–500 °C) and Si (Ge) film thickness (50–200 nm). We consider the experimental results within the framework of a model based on the assumption that the migration of hydrogen atoms from the dielectric Si_3N_4 into the growing Si and Ge films is controlled by the difference in chemical potentials of hydrogen atoms in the dielectric layer and the Si(Ge) film and is not related to thermal diffusion. This process occurs only during the growth of Si and Ge films and is interrupted with the cessation of growth and the alignment of chemical potential levels.

DOI: 10.31857/S004445102405e043

1. INTRODUCTION

Silicon nitride (Si_3N_4) is widely used in micro- and optoelectronics, as dielectric layers, antireflective coatings and passivation layers of solar cells [1–4]. Although the main method of its production is low-temperature (below 450 °C) plasma-enhanced chemical vapor deposition (PECVD), Si_3N_4 layers obtained using the low-pressure chemical vapor deposition (LPCVD) at high temperature (700–850 °C) have a number of advantages. Si_3N_4 films deposited by LPCVD have a nearly stoichiometric composition and a low content of hydrogen atoms, which improves their electrical parameters and thermal stability compared to Si_3N_4 films obtained using PECVD. The $\text{Si}_3\text{N}_4/\text{Si}$ protective coatings deposited by low-temperature methods are extensively used as a source of hydrogen atoms to prevent degradation of the electrical parameters of single-crystalline (c-Si), multi-crystalline (mc-Si) and amorphous (α -Si) silicon [2–5]. Hydrogen atoms can diffuse from the Si_3N_4 layer into the underlying Si layer and passivate broken Si bonds in a narrow interfacial region, thereby improving the electrical properties of the structures. [4, 5].

Studies of diffusion processes of hydrogen atoms into the underlying SiO_2 or Si layers has shown that

hydrogen atoms do not migrate across the $\text{Si}_3\text{N}_4/\text{SiO}_2$ boundary somewhat noticeably, and only an increase in the annealing temperature to 1000 °C leads to a slight increase in the content of hydrogen atoms in SiO_2 , but only if the Si_3N_4 layer had been applied by PECVD [6]. Annealing of $\text{Si}_3\text{N}_4/\text{c-Si}$ structures in the temperature range of 500–1000 °C does not lead to an increase in the concentration of hydrogen atoms in the c-Si layer [7, 8]. The possible diffusion of hydrogen atoms across the $\text{Si}_3\text{N}_4/\alpha\text{-Si}$ or mc-Si interface was studied in order to improve the electrical parameters of solar cells, e.g., those with a protective Si_3N_4 coating. The investigation of such structures is complicated since Si_3N_4 , $\alpha\text{-Si}$ or mc-Si layers are hydrogenated. Currently, the process of diffusion of hydrogen atoms has been studied in layers of polycrystalline and amorphous Si [9] obtained by plasma enhanced chemical vapor deposition. The content of hydrogen atoms can reach 25 % in such films [7].

Another widely used method for producing hydrogenated films is the implantation of hydrogen atoms into a silicon substrate. It is established that the activation energy of the diffusion of hydrogen atoms is approximately equal to 1.5 eV [9–11], which exceeds the Si–H binding energy amounting to approximately 3 eV [12]. The proposed diffusion mechanism is movement

* E-mail: arapkina@kapella.gpi.ru

through interstitial states. [9, 10, 13–16]. The diffusion rate depends on the concentration of hydrogen atoms, temperature and the type of doping of the Si layer.

This article presents the results of a study of hydrogen atom diffusion from an LPCVD-deposited Si_3N_4 top layer of a $\text{Si}_3\text{N}_4/\text{SiO}_2/\text{Si}$ (001) substrate into a growing film of polycrystalline (poly) or amorphous (α) Si or Ge layers. Such substrates are usually utilized in the production of photodetector structures [17] and can contain up to 8 % of H atoms [7, 18, 19]. Previously [17, 20–22], we have presented the results of a study of the diffusion of hydrogen atoms from dielectric layers (Si_3N_4 and SiO_2) into growing poly- and α -Si and Ge films for a wide range of growth temperatures (30–650 °C). It has been shown that the diffusion process occurs already at a low growth temperature (30 °C), i.e. when its thermal stimulation is absent.

In the current work, the results of an exploration of hydrogen diffusion in poly- and α -Si and Ge films of different thicknesses are presented. It is shown that the diffusion of hydrogen atoms depends on the thickness of the growing layers of Si and Ge. A model of hydrogen atom diffusion is proposed that takes into account the film deposition temperature and its thickness. The studies were carried out using the methods of reflected high-energy electron diffraction (RHEED) and Fourier transform infrared spectroscopy (FTIR).

2. EXPERIMENTAL

Experimental samples with thin Si or Ge layers deposited by molecular beam deposition (MBE) on $\text{Si}_3\text{N}_4/\text{SiO}_2/\text{Si}$ (001) substrates were prepared. The 530 nm thick SiO_2 layers were applied on silicon wafers using thermal oxidation, while 170 nm thick Si_3N_4 ones were formed by LPCVD at 750 °C. The temperatures of the processes of formation of SiO_2 and Si_3N_4 layers exceeded the growth temperatures of Si and Ge films. More detailed information on the methods and modes of manufacturing the dielectric layers of the substrates and the preliminary chemical preparation is presented in the works [20, 21].

After transferring the samples to ultra-high vacuum conditions, preliminary heat treatment of the substrates was carried out at a temperature of 600 °C, which lasted for 6 hours. Si and Ge films were deposited using electron beam evaporation sources in the EVA 32 growth chamber of the Riber SSC 2 ultra-high vacuum center. The growth temperatures of α - and poly-Si and Ge layers of different thicknesses (50, 100 and 200 nm) were 30 and 500 °C. Samples with layer thicknesses of

50 and 100 nm, grown at 500 °C, were additionally kept at the growth temperature after shutting off the flux of Si (Ge) atoms for the total duration of the process to be equal for all the samples. The deposition rates of Si and Ge films were $\sim 0.3 \text{ \AA}/\text{c}$.

In Fig. 1, a scheme of layer arrangement in the studied samples is presented. More details about the growth processes and control methods can be found in the works [20, 21]. The main experimental techniques were *in-situ* reflected high-energy electron diffraction (RHEED) using an RH20 RHEED tool (Staib Instruments) and Fourier transform infrared spectroscopy (FTIR). IR transmission and reflection spectra were registered using a vacuum IFS-66v/S spectrometer (Bruker) in the range of 400–4600 cm^{-1} with the spectral resolution of 10 cm^{-1} [20, 21]. The spectrometer was evacuated to the pressure of 2 mbar in order to reduce the influence of carbon dioxide and water vapor. IR absorption bands were decomposed into spectral components; peaks with a Gaussian profile were used for deconvolution.

3. RESULTS

According to the study performed *in situ* using RHEED, all Si and Ge films grown at 500 °C have a polycrystalline structure, whilst at 30 °C, an amorphous one. At the initial stages of growth of polycrystalline films, the diffraction patterns consisted of continuous wide rings (Fig. 2a), yet as the thickness of the growing layer increased, the rings narrowed and gaps appeared in them (Fig. 2b). Thus, at the initial stage of growth, the polycrystalline film was formed by small grains without ordering in the direction of growth. Then a gradual enlargement of grain sizes occurred and some preferential growth direction appeared. Images of amorphous and polycrystalline Si films obtained by transmission electron microscopy (TEM) are shown in Fig. 3. The polycrystalline Si film (Fig. 3a) has a structure in the form of columnar grains, starting at the interface with the Si_3N_4 dielectric layer and increasing their lateral size as the thickness of the growing film increases, which is typical for the growth of polycrystalline films at temperatures that ensure rapid diffusion of Si atoms over the growth surface. The region of the polycrystalline Si film adjacent to the interface with the substrate has the largest number of defects. Fig. 3b shows a structure with an amorphous Si layer grown at 30 °C under conditions of slow diffusion of atoms over the growth surface.

The study of IR spectra has shown that the main absorption bands are associated with vibrations of the Si–O, Si–N and N–H bonds in the initial $\text{Si}_3\text{N}_4/\text{SiO}_2/\text{Si}$ (001) substrate. Preliminary heat treatment of the substrates at 600 °C for 6 hours did not result in any changes in the spectra. Fig. 4 shows the IR absorption spectra in the spectral range of 400–1300 cm^{-1} for the structures with Si and Ge layers grown at 30 and 500 °C. All the spectra are characterized by the presence of two broad absorption bands at about 825 cm^{-1} and 1090 cm^{-1} , associated with vibrations of the Si–O bonds in the $\text{Si}_3\text{N}_4/\text{SiO}_2/\text{Si}$ (001) substrate. Deconvolution of the IR spectra has shown that it is possible to identify absorption bands related to vibrations of Si–O ($\sim 735, 805, 1075, 1100$ and 1190 cm^{-1}), Si–N ($\sim 860 \text{ cm}^{-1}$) and N–H ($\sim 1150 \text{ cm}^{-1}$) bonds in the $\text{Si}_3\text{N}_4/\text{SiO}_2/\text{Si}$ (001) substrate [23,24] and vibrations of Si–O bonds in the oxynitride layer ($\sim 960 \text{ cm}^{-1}$) located on the Si_3N_4 surface [21]. The main changes in the spectra are associated with the absorption bands of Si–N ($\sim 860 \text{ cm}^{-1}$), N–H ($\sim 1150 \text{ cm}^{-1}$) and Si–O ($\sim 960 \text{ cm}^{-1}$) (highlighted in bold in Fig. 4). The application of the Si and Ge films has different effects on the change in the intensity of these bands. In the structures with Si layers, the intensity of the Si–N band increases with increasing growth temperature, whereas the intensity of the N–H band decreases. In structures with Ge layers, the intensity of the absorption bands of Si–N, N–H and Si–O decreases with an increase in growth temperature. (Fig. 4).

Fig. 5 shows the IR absorption spectra of structures with poly-Si and poly-Ge layers of different thicknesses grown at 500 °C. Changes in the intensity of the absorption bands associated with vibrations of the Si–N ($\sim 860 \text{ cm}^{-1}$), N–H ($\sim 1150 \text{ cm}^{-1}$) and Si–O ($\sim 960 \text{ cm}^{-1}$) bonds (highlighted in bold in Fig. 5) increase with increasing layer thickness. The main differences between structures with Si and Ge layers related to the changes in the intensities of the Si–N and Si–O absorption bands. At the samples with poly-Si, with increasing film thickness, a decrease in the intensity of the N–H absorption bands and an increase in the intensity of the Si–N absorption bands are observed (Fig. 5a), which corresponds to the result shown in Fig. 4a. For the structures with poly-Ge, a decrease in the intensity of the Si–O absorption band is added; in addition, it cannot be unambiguously determined for these samples whether the intensity of the Si–N band changes (Fig. 5b). Fig. 6 shows the change in the intensity of the Si–N, N–H and Si–O absorption bands derived by deconvolution of the spectra presented in Fig. 5 and

the spectra for the structures with α -Ge. In the structures with poly-Si and poly-Ge, the intensity of the N–H band ($\sim 1150 \text{ cm}^{-1}$) decreases with an increase in the thickness of the deposited films. The intensity of the Si–O absorption band ($\sim 960 \text{ cm}^{-1}$) decreases significantly only in the case of structures with Ge layers. The absorption in the Si–N band ($\sim 860 \text{ cm}^{-1}$) increases stronger in the samples with Si layers than in the samples with Ge layers. Comparison of the structures with α -Ge and poly-Ge shows that the intensity of the Si–N absorption band ($\sim 860 \text{ cm}^{-1}$) increases more during the low-temperature growth (30 °C) than during the high-temperature growth (500 °C).

4. DISCUSSION

To explain the observed results, we use the hydrogen atom diffusion model proposed in [9, 10, 13–16] for amorphous Si and Ge films. Temperature conditions for the growth of Si and Ge layers are not favorable for the thermal diffusion of hydrogen atoms. The activation energy of diffusion of hydrogen atoms in α -Si and α -Ge is approximately 1.5 eV [10, 25], whilst the binding energies of N–H and Si–H bonds are approximately 4 and 3 eV [12]. In the proposed model, the diffusion of hydrogen atoms is considered as their movement through interstitial states with the formation of bonds with two silicon (germanium) atoms located at the lattice sites, Si–H–Si (Ge–H–Ge),¹ due to the breaking of “weak” Si–Si (Ge–Ge) bonds. The number of “weak” Si–Si (Ge–Ge) bonds increases with increasing disorder in the crystal lattice. The Si–H and Ge–H bonds are traps limiting the diffusion rate; they form by the interaction of a hydrogen atom with a Si (Ge) atom having a dangling bond. The main concept in the model is the chemical potential of hydrogen atoms μ_{H} . Fig. 7 presents the energy diagram of the diffusion process of hydrogen atoms in Si (the right panel in Fig. 7a). The deepest level $E_{\text{Si–H}}$ (the state with the highest energy) belongs to one of the Si–H deep traps. They occupy levels below μ_{H} . The diffusion of hydrogen atoms occurs during the formation of Si–H–Si bonds, the energy level of which is located above μ_{H} (shallow energy level). This is the so-called transport level E_{TR} . If there are a sufficient number of “weak” Si–Si bonds in the crystal structure, then hydrogen atoms can transit from the μ_{H} level to the E_{TR} , and their diffusion is observed. The position of μ_{H} depends on the concentration of hydrogen atoms. The higher it is, the

1. This arrangement is often referred to as “bond-centered-defect” in the literature.

higher the μ_H position (lower the energy). This is indirectly confirmed by the results of Ref. [9], in which an increase in the diffusion coefficient was observed with an increase in the concentration of hydrogen atoms in Si. In the structures formed by layers with different contents of hydrogen atoms, the μ_H levels should align and diffusion of hydrogen atoms should be observed.

In the studied structures, the highest concentration of hydrogen atoms is in the dielectric Si_3N_4 layer, where the position of μ_H is higher than in the growing Si layer, yet to start diffusion, it is necessary to overcome a high energy barrier (Fig. 7a, the left panel), since hydrogen atoms are bonded as N–H. The initial positions of the energy levels in Si_3N_4 and Si layers are shown in Fig. 7a. With the beginning of growth (Fig. 7b), due to the different positions of μ_H in Si_3N_4 and Si, the transition of hydrogen atoms occurs from the Si_3N_4 layer to the Si layer. A new position of μ_H sets up (alignment occurs). If the growth of the Si layer (designated as Si(H) in Fig. 7b) ceases, then the transition of hydrogen atoms from Si_3N_4 also stops. If the growth continues, a region with a lower position of μ_H forms at the growth surface (designated as +Si in Fig. 7c), and the position of μ_H should level off (lower) throughout the grown Si layer. The newly emerging difference in chemical potential values between the Si_3N_4 and Si layers causes hydrogen atoms to move from the Si_3N_4 layer to the Si layer, and μ_H occupies a new position (Fig. 7d).

Thus, the diffusion of hydrogen atoms occurs only directly during the growth of the Si layer, which leads to the dependence on its thickness. Let us consider the growth temperature effect on this process. With an increase in the growth temperature and the transition to a polycrystalline structure of the Si and Ge layers, due to the increased vibrations of the lattice atoms or the increase in disorder in the regions of grain boundaries, the number of “weak” Si–Si (Ge–Ge) bonds increases and the thermal diffusion of hydrogen atoms accelerates, which leads to a more rapid leveling of the chemical potential μ_H in the growing Si (Ge) film. Another factor intensifying hydrogen diffusion may be a different diffusion mechanism in the single-crystal part of the polycrystalline structure. It is known that the activation energy of hydrogen diffusion in c-Si is about 0.48 eV [26] and the value of the diffusion coefficient decreases with an increase in the content of hydrogen atoms [27]. Also, thermal desorption of hydrogen atoms from the near surface area might occur at high growth temperatures [25], which lowers the μ_H level and promotes the transition of hydrogen atoms into the growing Si film [9, 28].

In the IR spectra of structures with 50 nm thick Ge layers (Fig. 6b, c), a more noticeable decrease in the intensity of the N–H absorption bands is observed in the samples with the amorphous films. This may be related to the structure of growing films [22]. The growth of polycrystalline layers begins with the formation of small grains with a large proportion of grain boundaries in the volume of the film, where likely a large number of atoms with dangling bonds may be contained, which are deep traps for hydrogen atoms. As the film thickness increases, their number decreases, which enhances the diffusion of hydrogen atoms. As is evident from the IR spectra of structures with polycrystalline layers of Si and Ge [17, 20, 21], no formation of Si–H_x and Ge–H_x absorption bands was observed in poly-Si and poly-Ge. This may be due to their insufficient concentration or the formation of Si–H (Ge–H) bonds, which are not IR-active.

The deposition of Si (Ge) layers changed the intensity of the Si–N ($\sim 860 \text{ cm}^{-1}$) and Si–O ($\sim 960 \text{ cm}^{-1}$) absorption bands. As shown by the results of a study using the method of photoelectron spectroscopy with layer-by-layer etching [21], simultaneously with the outmigration of hydrogen atoms from the dielectric film, counter diffusion of Si (Ge) atoms into it occurs. The change in the intensity of the Si–N absorption band is associated with a decrease in the concentration of hydrogen atoms in Si_3N_4 accompanied by the rupture of N–H bonds and the formation of Si–N bonds instead. In the case of growth of a Si layer, additional Si atoms arrive from the growing film, and the number of Si–N bonds increases. When growing Ge films, Ge–N bonds are formed, i.e. there is no additional source of Si atoms. Another factor in changing the intensity of the Si–N absorption band is that the introduction of additional Si atoms does not introduce distortions into the Si_3N_4 structure and can improve the order in it, while Ge atoms, which have a larger size, can introduce such distortions. The weakening of the absorption in the Si–O band ($\sim 960 \text{ cm}^{-1}$) is associated with the destruction of these bonds in the oxynitride layer during the diffusion of Ge atoms through it [21].

5. CONCLUSION

The polycrystalline and amorphous Si and Ge films grown on $\text{Si}_3\text{N}_4/\text{SiO}_2/\text{Si}(001)$ dielectric substrates have been explored by means of RHEED and FTIR spectroscopy. As a result of the deposition of Si and Ge layers, a significant decrease in the intensity of the absorption bands associated with vibrations of N–

H bonds was observed, which increased with increasing thickness of the growing films. To explain the experimental results, it has been proposed to use a model based on the assumption that, in the absence of thermal diffusion, the transition of hydrogen atoms from the Si_3N_4 dielectric layer to the growing Si or Ge film is controlled by the different positions of the chemical potential levels of hydrogen atoms in them. The difference in the chemical potentials of hydrogen atoms in Si_3N_4 and the Si (Ge) film is maintained only during the growth of the films. This explains the dependence of the intensity of the IR absorption bands on the film thickness. With an increase in the film growth temperature, the process of the chemical potential leveling in Si_3N_4 and Si (Ge) accelerates owing to the possible thermal diffusion of hydrogen atoms.

REFERENCES

1. B. J. Hallam, P. G. Hamer, A. M. C. Wenham, C. E. Chan, B. V. Stefani, and S. Wenham, *Prog. Photovolt. Res. Appl.* **1**, 1217 (2020), doi: 10.1002/pip.3240.
2. W. Soppe, H. Rieffe, and A. Weeber, *Prog. Photovolt. Res. Appl.* **13**, 551 (2005), doi: 10.1002/pip.611.
3. R. S. Bonilla, B. Hoex, P. Hamer, and P. R. Wilshaw, *Phys. Status Solidi (a)* **214**, 1700293 (2017), doi: 10.1002/pssa.201700293.
4. M. Z. Rahman, *Renew. Sustain. Energy Rev.* **30**, 734 (2014), doi: 10.1016/j.rser.2013.11.025.
5. A. G. Aberle, *Sol. Energy Mater. Sol. Cells* **65**, 239 (2001), doi: 10.1016/S0927-0248(00)00099-4.
6. J. Z. Xie, S. P. Murarka, X. S. Guo, and W. A. Lanford, *J. Vac. Sci. Technol. B* **7**, 150 (1989), doi: 10.1116/1.584707.
7. P. S. Peercy, H. J. Stein, B. L. Doyle, and S. T. Picraux, *J. Electron. Mater.* **8**, 11 (1979), doi: 10.1007/BF02655637.
8. C. Boehme and G. Lucovsky, *J. Appl. Phys.* **88**, 6055 (2000), doi: 10.1063/1.1321730.
9. W. Beyer, *Phys. Stat. Sol. (a)* **213**, 1661 (2016), doi: 10.1002/pssa.201532976.
10. W. Beyer, *Sol. Energy Mater. Sol. Cells* **78**, 235 (2003), doi: 10.1016/S0927-0248(02)00438-5.
11. C. G. V. D. Walle and R. A. Street, *Mat. Res. Soc. Symp. Proc.* **377**, 389 (1995), doi: 10.1557/PROC-377-389.
12. J. Robertson, *Philos. Mag. B* **69**, 307 (1994), doi: 10.1080/01418639408240111.
13. R. A. Street, *Phys. Rev. B* **43**, 2454 (1991), doi: 10.1103/PhysRevB.43.2454.
14. P. V. Santos, N. M. Johnson, R. A. Street, M. Hack, R. Thompson, and C. C. Tsai, *Phys. Rev. B* **47**, 10244 (1993), doi: 10.1103/PhysRevB.47.10244.
15. W. B. Jackson and C. C. Tsai, *Phys. Rev. B* **45**, 6564 (1992), doi: 10.1103/PhysRevB.45.6564.
16. S. C. Deane and M. J. Powell, *J. Non-Cryst. Solids* **198–200**, 295 (1996), doi: 10.1016/0022-3093(95)00690-7.
17. K. V. Chizh, L. V. Arapkina, V. P. Dubkov, D. B. Stavrovsky, and V. A. Yuryev, *M. S. Storozhevykh, Optoelectron. Instrum. Data Process.* **58**(6), 616 (2022), doi: 10.3103/S8756699022060036.
18. P. Paduscek and P. Eichinger, *Appl. Phys. Lett.* **36**, 62 (1980), doi: 10.1063/1.91317.
19. H. J. Stein, *J. Electron. Mater.* **5**, 161 (1976), doi: 10.1007/BF02652901.
20. K. V. Chizh, L. V. Arapkina, D. B. Stavrovsky, P. I. Gaiduk, and V. A. Yuryev, *Mater. Sci. Semicond. Process.* **99**, 78 (2019), doi: 10.1016/j.mssp.2024.108659.
21. L. V. Arapkina, K. V. Chizh, D. B. Stavrovskii, V. P. Dubkov, E. P. Lazareva, and V. A. Yuryev, *Sol. Energy Mater. Sol. Cells* **230**, 111231 (2021), doi: 10.1016/S0927-0248(00)00076-3.
22. M. S. Storozhevykh, V. P. Dubkov, L. V. Arapkina, K. V. Chizh, S. A. Mironov, V. A. Chapnin, and V. A. Yuryev, *Proc. SPIE* **10248**, 102480O (2017), doi: 10.1117/12.2265882.
23. D. Davazoglou and V. E. Vamvakas, *J. Electrochem. Soc.* **150**, F90 (2003), doi: 10.1149/1.1562601.
24. E. A. Taft, *J. Electrochem. Soc.* **118**, 1341 (1971), doi: 10.1149/1.2408318.
25. W. Beyer, J. Herion, H. Wagner, and U. Zastrow, *Philos. Mag. B* **63**, 269 (1991), doi: 10.1080/01418639108224444.
26. A. Van Wieringen and N. Warmoltz, *Physica* **22**, 849 (1956), doi: 10.1016/S0031-8914(56)90039-8.
27. Y. L. Huang, Y. Ma, R. Job, and A. G. Ulyashin, *J. Appl. Phys.* **96**, 7080 (2004), doi: 10.1063/1.1812379.
28. W. Beyer, *J. Non-Cryst. Solids* **198–200**, 40 (1996), doi: 10.1016/0022-3093(95)00652-4.

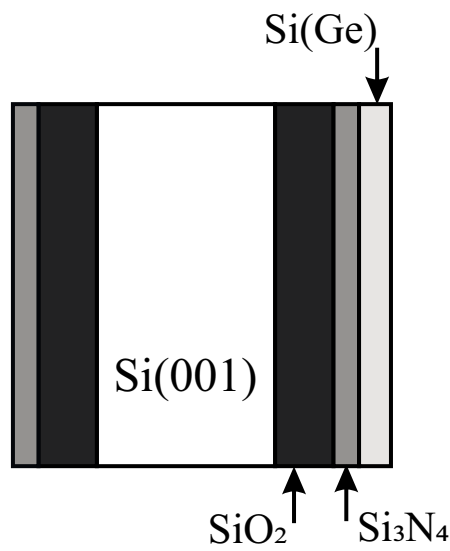


Fig. 1. Layer arrangement scheme in the studied samples

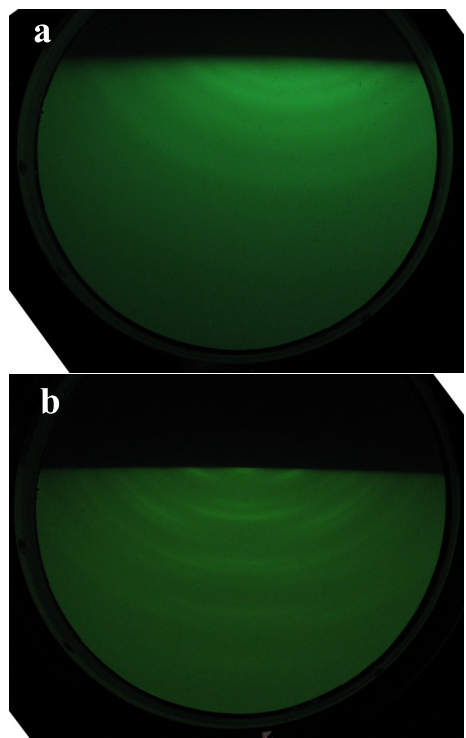


Fig. 2. (Color online) Diffraction patterns of the surface of a polycrystalline Si layer with a thickness of (a) 20 Å and (b) 200 nm

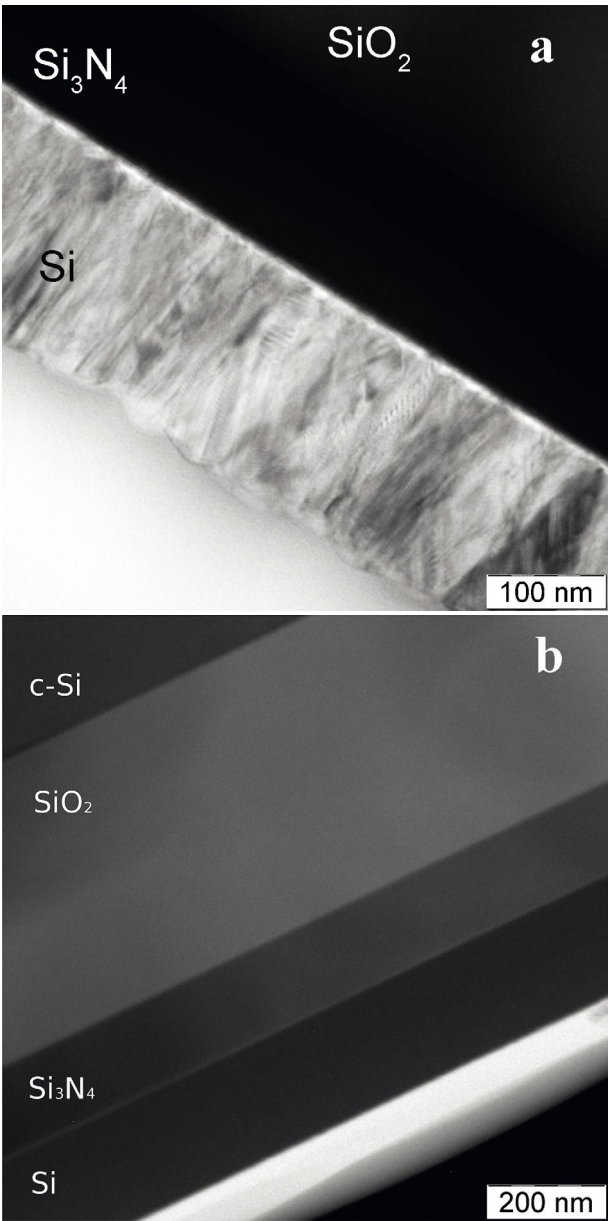


Fig. 3. TEM images of (a) polycrystalline and (b) amorphous Si films; the substrate is on top of the image

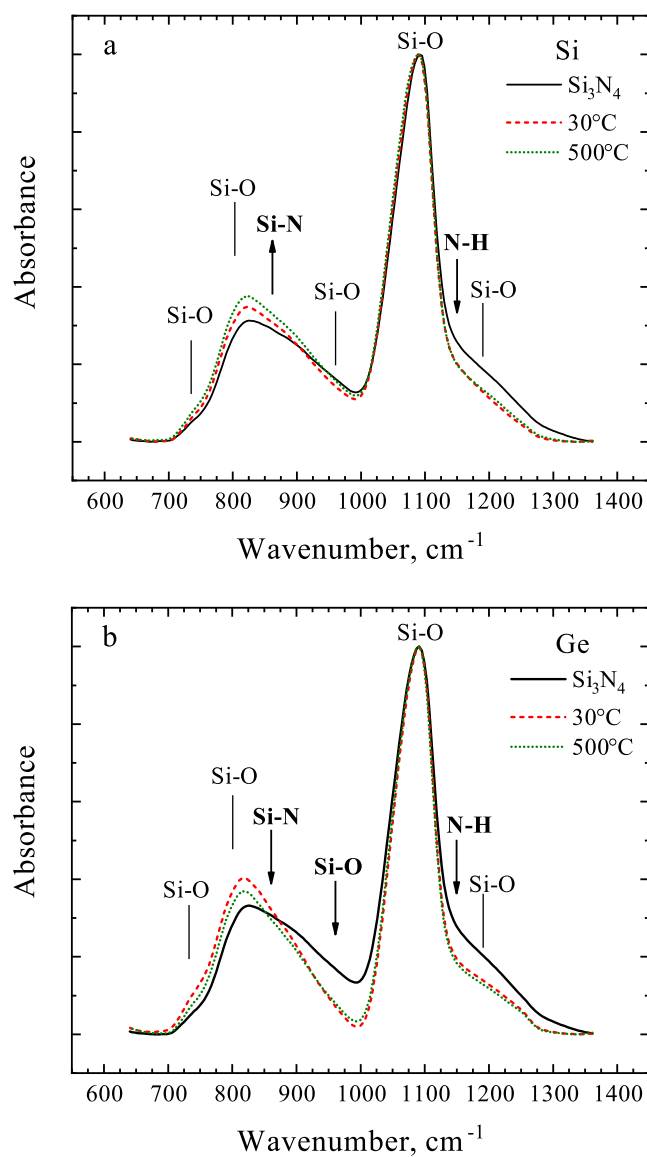


Fig. 4. (Color online) IR absorption spectra of 200 nm thick Si (a) and Ge (b) layers grown at 30 and 500°C on $\text{Si}_3\text{N}_4/\text{SiO}_2/\text{Si}(001)$ substrates; the spectra are normalized to the maximum intensity of the Si-O absorption band at $\sim 1100 \text{ cm}^{-1}$; the substrate spectrum is designated as Si_3N_4

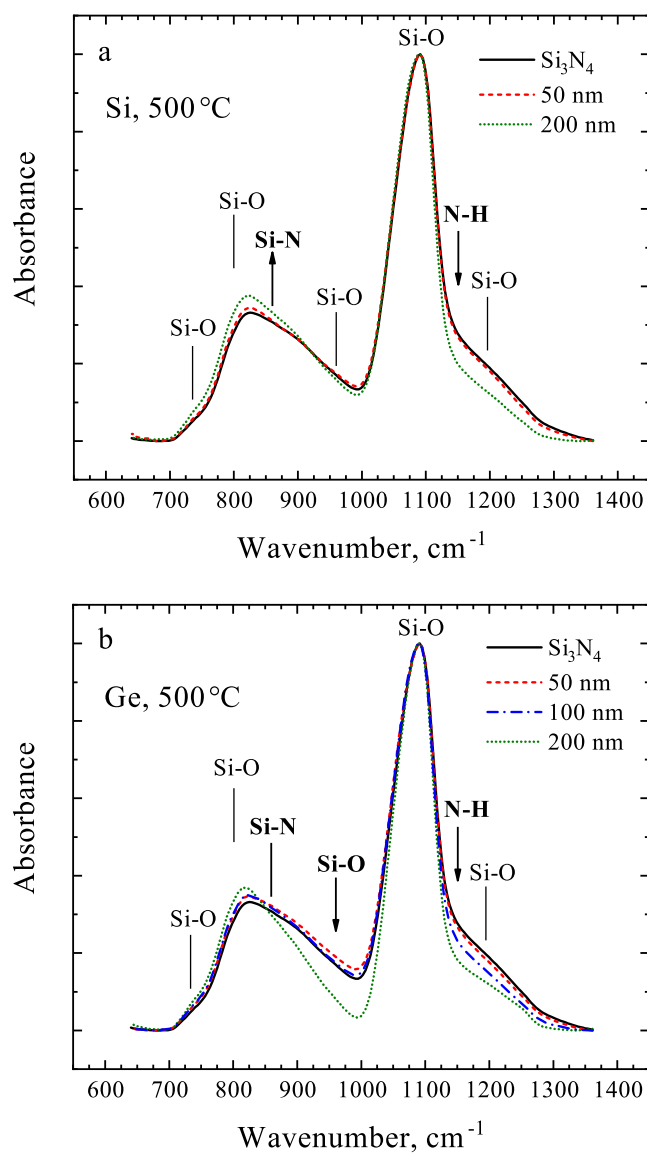


Fig. 5. (Color online) IR absorption spectra of Si (a) and Ge (b) layers of different thickness (50, 100 and 200 nm) grown at 500°C on $\text{Si}_3\text{N}_4/\text{SiO}_2/\text{Si}(001)$ substrates; the spectra are normalized to the maximum intensity of the Si-O absorption band at $\sim 1100 \text{ cm}^{-1}$; the substrate spectrum is designated as Si_3N_4

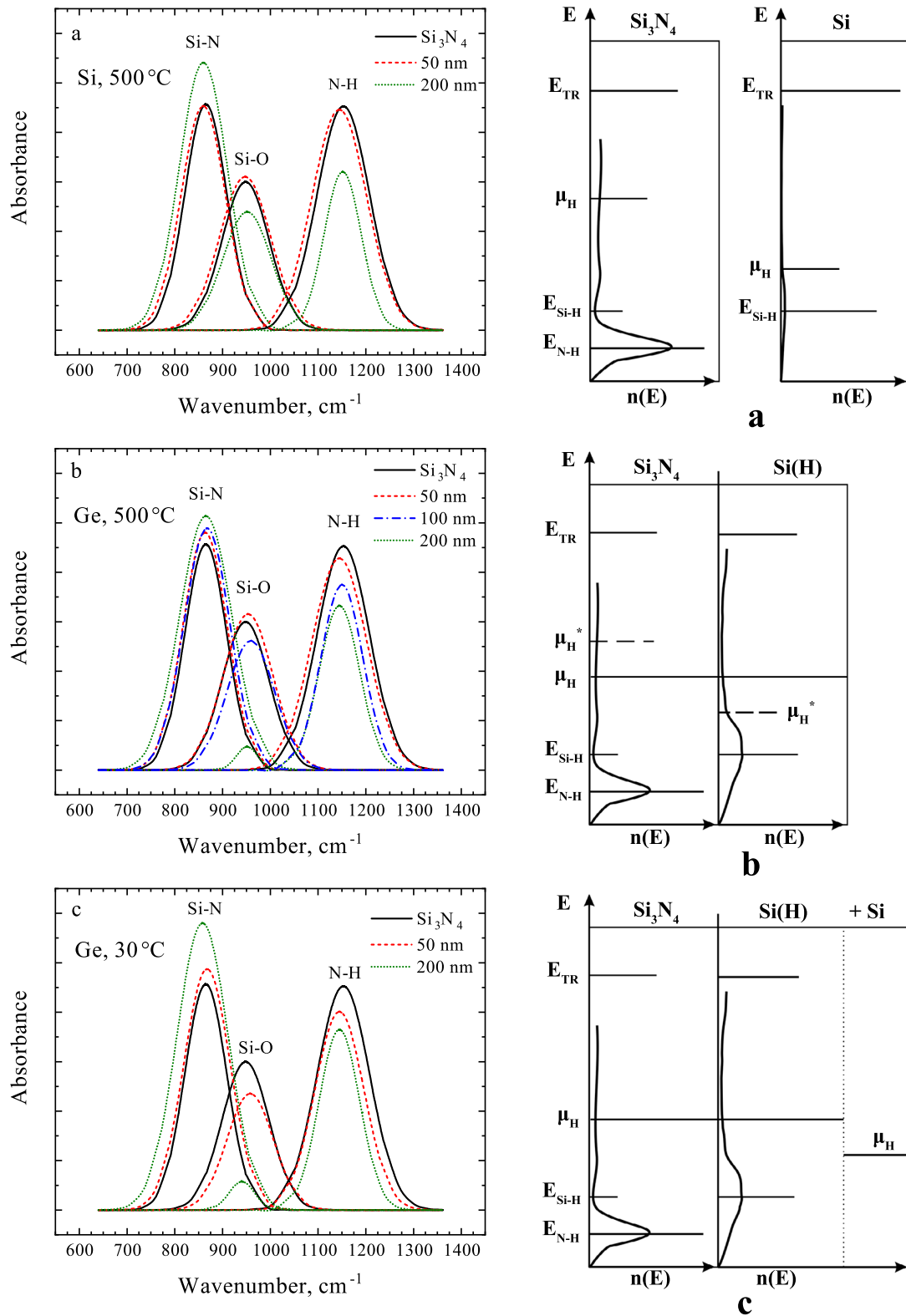


Fig. 6. (Color online) Changes in the intensity of absorption bands associated with vibrations of Si-N ($\sim 860\text{ cm}^{-1}$), N-H ($\sim 1150\text{ cm}^{-1}$) and Si-O ($\sim 960\text{ cm}^{-1}$) bonds as a result of deposition of layers of (a) polycrystalline Si, (b) polycrystalline and (c) amorphous Ge on $\text{Si}_3\text{N}_4/\text{SiO}_2/\text{Si}(001)$ substrates; the spectra of the substrates are designated as Si_3N_4

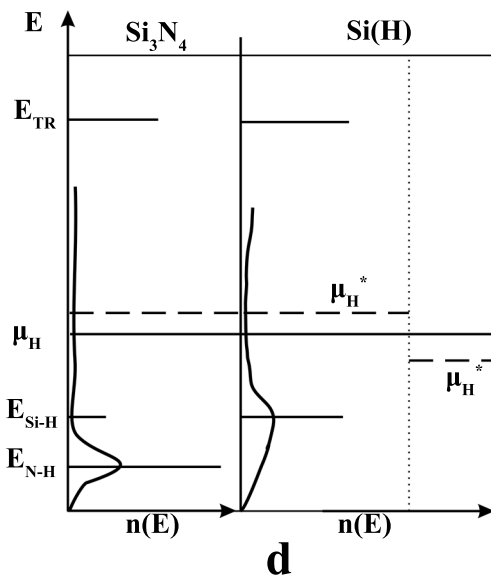


Fig. 7. Energy scheme of the process of diffusion of hydrogen atoms from a dielectric substrate (Si_3N_4) into a growing Si layer: (a) initial states of Si_3N_4 (left panel) and Si (right panel); (b) alignment of the μ_{H} position, formation of a Si(H) layer; (c) continuation of growth and addition of a $+\text{Si}$ layer; (d) alignment of the μ_{H} position; μ_{H}^* is the initial position of the chemical potential before alignment